

Multiscale cardiovascular modeling approach to assess arterial perfusion during atrial fibrillation

Original

Multiscale cardiovascular modeling approach to assess arterial perfusion during atrial fibrillation / Congiu, L., Scarsoglio, S., Ridolfi, L.. - 9:(2025). (Nineth National Congress of Bioengineering Palermo (Ita) 16-18 June, 2025).

Availability:

This version is available at: 11583/3009342 since: 2026-03-28T21:45:38Z

Publisher:

Pàtron editore

Published

DOI:

Terms of use:

This article is made available under terms and conditions as specified in the corresponding bibliographic description in the repository

Publisher copyright

(Article begins on next page)

Multiscale cardiovascular modeling approach to assess arterial perfusion during atrial fibrillation

Luca Congiu¹, Stefania Scarsoglio^{1,2}, Luca Ridolfi^{2,3}

¹*Department of Mechanical and Aerospace Engineering, Politecnico di Torino*

²*PolitoBioMed Lab, Politecnico di Torino*

³*Department of Environmental, Land and Infrastructure Engineering, Politecnico di Torino*

Abstract—Atrial fibrillation (AF) is the most common tachyarrhythmia, causing faster and irregular beating, as well as inhibiting the normal cardiac contractile function. We aim to develop a stochastic multiscale modeling of the cardiovascular system to investigate the AF impact on the arterial perfusion along the aorta. The contractility reduction and the irregular beating induce a high variability of the beat-averaged values of flow rate and pressure, as well as a reduction of the mean arterial perfusion that worsens from proximal to distal circulation. Present results can contribute explaining hemodynamic mechanisms underlying the augmented ischemic risk induced by AF in the mesenteric and renal vascular regions.

Keywords—Atrial fibrillation, multiscale cardiovascular model, arterial perfusion, computational hemodynamics

I. INTRODUCTION

Atrial fibrillation (AF) is the most common cardiac arrhythmia inducing faster and irregular heart beating (RR), counting about 60 million people affected worldwide [1] and with an incidence expected to double in the next years due to the increasing life expectancy [2]. AF induces a number of disabling symptoms - such as palpitations, chest discomfort, reduced physical capacity and cardiac efficiency - and has been more recently associated to a higher risk of cognitive decline [3].

Moreover, even if AF is believed to be a risk factor for mesenteric and renal ischemia [4, 5], apart from an increased probability of embolism, the underlying mechanisms linking AF to low gastrointestinal perfusion remain still unclear. The existing literature indeed lacks a thorough examination of the effects of AF on abdominal organ perfusion, as most studies have primarily focused on myocardial and cerebral perfusion.

We here propose a validated 0D-1D multiscale cardiovascular model [6-10] to investigate the AF impact along the aorta and the main gastrointestinal bifurcations. We considered two representative configurations of sinus rhythm (SR) and AF imposed on a generic healthy young patient, by simulating for each condition 2000 beats to guarantee the statistical stationarity of the results. SR was simulated at the common resting time-correlated beating (mean heart rate, HR: 70 bpm), AF configuration accounted for its most typical features: (i) accelerated, variable and uncorrelated beating (mean HR: 90 bpm); (ii) absence of atrial contraction, and (iii) ventricular systolic dysfunction. The comparison between SR and AF outcomes provide mechanistic hints into the role of AF in the altered arterial blood flow.

II. METHODS

A. Cardiovascular multiscale model: general description

A multiscale-closed loop cardiovascular model was exploited for conducting an investigation of the effect of AF on the hemodynamic in different sites of the aorta. The model has been extensively used and validated in previous works, aiming to study the effect of cardiac deficits, extreme environmental conditions, such as microgravity, and posture changes on the cardiovascular system [11-13]. The model includes a 1D representation of the arterial circulation coupled with several 0D compartments that describe the peripheral, venous, cardiopulmonary and cerebro-ocular circulations. The model is completed with a mathematical description of the baroreceptor, cardiopulmonary, cerebral-autoregulation and CO₂ reactivity regulatory mechanisms. The cardiopulmonary circulation is described by a lumped parameter model of the four chambers, valves and pulmonary circulation. Cardiac contraction is modelled by employing a normalized-shape elastance function, with proper values of maxima (E_{max}) and minima elastance (E_{min}) values associated to each chamber. Valves dynamics are implemented with four non-ideal diodes that consider different effects such as tissue friction and the influence of downstream vortexes [7].

B. SR and AF features

The model is representative of a 25 years old male subject, free of cardiovascular diseases. This baseline configuration was used to simulate the same generic subject in SR and AF conditions. Artificially-built RR intervals were constructed to force the correct beating rhythm in the two cases [7,9,10].

RR intervals in SR (RR_{SR}) were generated from a correlated pink Gaussian distribution, with mean value $\mu_{SR} = 0.86$ s (HR = 70bpm) and coefficient of variation $cv_{SR} = 0.07$. The AF is characterized by an irregular sequence of RR intervals, whose probability density function is defined by the superposition of a correlated Gaussian distribution and an uncorrelated exponential distribution. The RR_{AF} was extracted by the resulting exponentially-modified Gaussian distribution, imposing $\mu_{AF} = 0.67$ s (HR = 90 bpm), to take into account the faster heart rate commonly observed in AF patients, $cv_{AF} = 0.26$ and rate parameter $\gamma = 6$ Hz.

To obtain a faithful representation of a typical case of AF two more features were considered. First, AF patients present

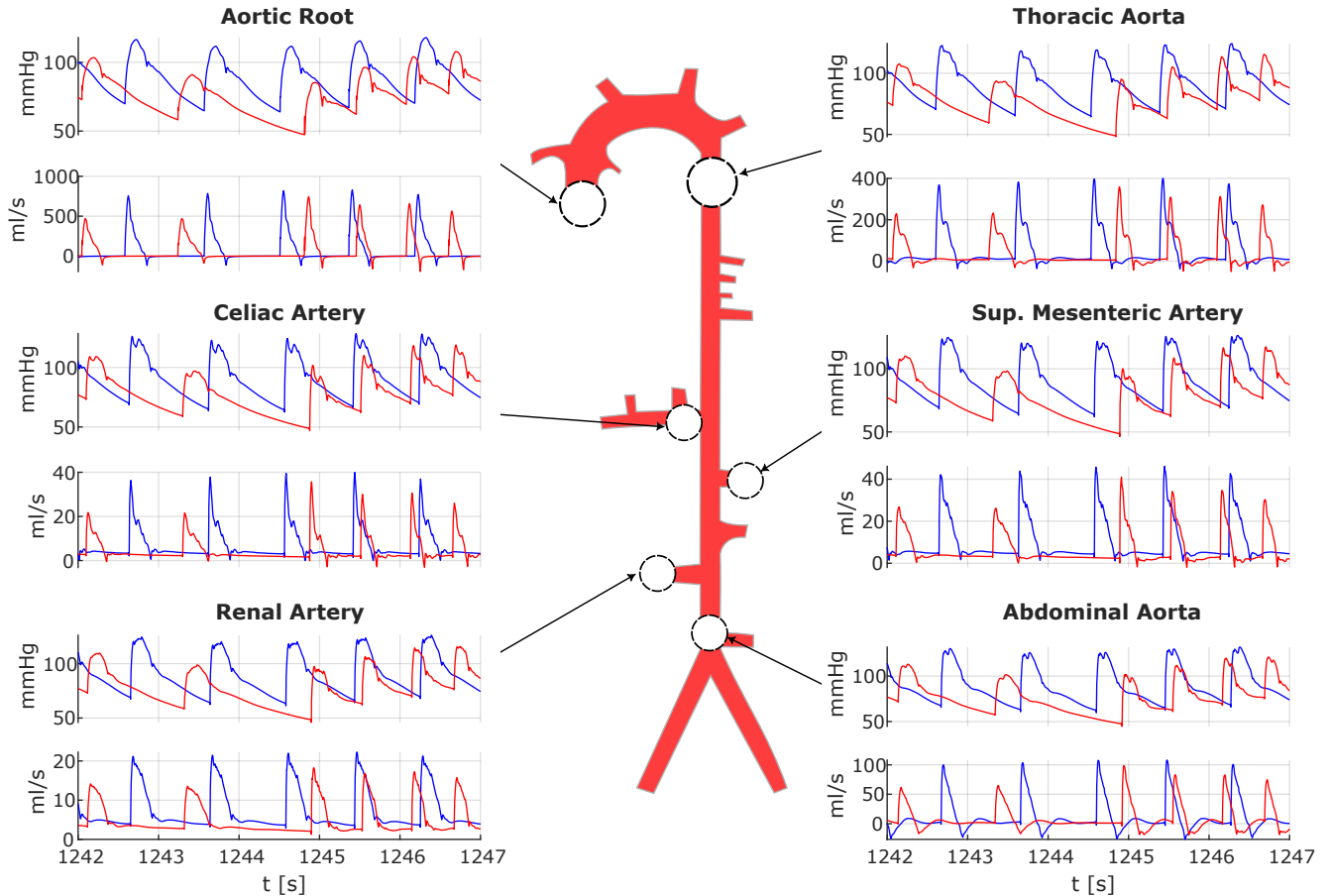


Fig. 1: Schematic of the aorta pathway. Six sites were chosen (aortic root, celiac artery, thoracic aorta, superior mesenteric artery, renal artery and abdominal aorta) and, for each site, representative time interval of the flow rate and pressure waveforms is displayed.

an impaired contribution of the atria to the ventricular filling due to the absence of atrial contraction. This was modeled by imposing a constant atrial elastance. Finally, reduced ventricular contractility, of both the right and left ventricle, is commonly observed in patients affected by AF. This feature was modelled by imposing a 40% reduction of the maximum elastance on both the ventricles.

For both the configurations, the first 50 beats were excluded as affected by numerical transient dynamics and the subsequent 2000 beats were collected to elaborate the relevant parameters.

III. RESULTS

A. Cardiac parameters

Three main cardiac parameters were computed to assess the cardiac efficiency in AF conditions: stroke volume (SV), defined as the difference between the end-diastolic and end-systolic left ventricular volumes, cardiac output (CO), defined as the product of SV and HR, and ejection fraction (EF), defined as the SV normalized to the end-diastolic left ventricular volume. Mean and standard deviation (std) were extracted for the three parameters and compared in the two cases. All three parameters were strongly affected by atrial fibrillation. Both SV and EF show a reduction in AF of -33.5% (from 76.3

to 50.7 ml) and -31.7% (From 61.2 to 42%) respectively in good agreement with literature values [7]. As the decrease of SV and EF is similar, we can infer that these reductions are mainly driven by an increase in the end-systolic left ventricular volume due to the reduction of the left ventricle E_{max} .

The reduction of SV in AF led to a consequent reduction of the CO (-10.8%) which, however, is mitigated by the higher HR imposed in AF condition. Overall, these results indicate a significant decline in the heart's ability to adequately perfuse body tissues in AF. The variability of the three variables, assessed with the std, exhibits a sharp increase of 226%, 114.6% and 142.6% for the CO, SV and EF respectively. The decrease of the mean values of the three cardiac parameters associated with the sharp increase in their variability highlights a condition characterized by the presence of several intervals of severe hypoperfusion which, if prolonged in time as in several cases of AF, can lead to substantial damage to the organs.

B. Arterial hemodynamics

To quantify whether the above described AF-induced cardiac dysfunction affect the arterial tree, we here focused on the aortic pathway, selecting six specific sites for analysis: the aortic root, thoracic aorta, and abdominal aorta – representing different

TABLE I: BEAT-TO-BEAT HEMODYNAMICS PARAMETERS

Artery	Variable	Mean			std		
		SR	AF	$\Delta\%$	SR	AF	$\Delta\%$
<i>Pressures</i>							
Aortic Root	PP	47.67	33.06	-30.65	2.41	5.71	136.68
	μ	90.74	86.73	-4.41	2.57	4.72	83.58
Thoracic Aorta	PP	54.48	40.34	-25.95	2.41	5.58	131.45
	μ	92.54	88.57	-4.29	2.56	4.70	83.50
Celiac Artery	PP	60.91	44.94	-26.22	2.40	5.51	129.50
	μ	92.57	88.73	-4.15	2.54	4.67	83.76
Renal Artery	PP	58.23	41.92	-28.01	2.41	5.63	134.10
	μ	91.59	88.06	-3.86	2.50	4.62	84.60
Sup. Mesenteric Artery	PP	58.69	43.49	-25.90	2.41	5.55	130.59
	μ	92.30	88.54	-4.07	2.53	4.65	83.98
Abdominal Aorta	PP	66.04	48.20	-27.02	2.33	5.76	147.11
	μ	91.31	87.60	-4.06	2.52	4.65	84.33
<i>Flow rates</i>							
Aortic Root	μ	83.26	71.69	-13.90	4.65	14.98	221.88
Thoracic Aorta	μ	54.44	44.20	-18.81	2.76	7.42	169.18
Celiac Artery	μ	7.28	5.86	-19.49	0.33	0.65	100.62
Renal Artery	μ	7.67	6.21	-19.02	0.32	0.63	92.63
Sup. Mesenteric Artery	μ	10.27	8.09	-21.24	0.49	0.97	97.54
Abdominal Aorta	μ	12.32	10.21	-17.11	0.63	1.70	171.06

Beat-averaged (μ) and pulse pressure (PP) pressure values are reported in mmHg. Beat-averaged (μ) flow rate values are expressed in ml/s.

segments of the main aortic pathway – and the right renal artery, celiac artery, and superior mesenteric artery – which were chosen to evaluate the renal and gastrointestinal perfusion.

1) *Pressure and flow rate waveforms*: Figure 1 shows, for each site, a time interval of the pressure and flow rate time-series representative of the behavior of the system in SR (blue curves) and AF (red curves). It is worth recalling that, the high variability of RR_{AF} can lead to sporadic beats with a particularly slow or fast HR, which is reflected in the peculiar waveforms observed in Figure 1. As highlighted in previous studies [8], the alternation of exceptionally long and short beats under AF conditions results in a characteristic pattern, where pressure declines during prolonged RR intervals, reaching lower systolic and diastolic values, and then gradually rises back to higher pressure levels during the sequent short beats. This pattern can be seen in all the pressure panels of Figure 1, highlighting that the effect of AF, starting from the aortic root, persists unaltered also in distal sections of the arterial tree.

Comparing pressure and flow rate waveforms we see that, in correspondence with the long decline of the pressure observed during long beats, the flow rate is completely impaired along the main path of the aorta (aortic root, thoracic aorta, abdominal aorta) and strongly reduced on the renal and gastrointestinal branches (celiac artery, renal artery, and mesenteric artery) as the diastole duration is markedly increased. Moreover, the low values of SV and CO are reflected in the lower peak values of the flow, highlighting the possible reduction in the perfusion capacity of the heart under AF conditions.

2) *Beat-to-beat analysis*: In order to quantitatively evaluate the influence of AF on arterial hemodynamics beat-averaged

(μ) and pulse pressure ($PP = P_{max} - P_{min}$) for each beat were extracted, for all six sites. For what concern the flow rates only the beat-averaged (μ) values were considered. Table 1 reports mean and std of the beat-averaged values of pressures and flow rates, and of the pulse pressures.

In all the sites, the mean and std of the beat-averaged pressure values show a moderate decrease (around -4%) and a strong increase (approximately 84%), respectively, highlighting an uniform influence of the AF along the aorta on the trend of the pressure waveforms, as observed qualitatively from figure 1. On the contrary, flow rate beat-averaged values show a more pronounced and less uniform decrease in the mean values. The higher decrements are observed in the renal and gastrointestinal perfusing arteries, with the highest reduction localized in the mesenteric artery (-21.2%). However, focusing on the std, we can notice that the renal, celiac and mesenteric arteries present a less marked increase in variability (+100.6% in the celiac artery) with respect to the main aorta pathway (+221.9% and +171% observed in the aortic root and abdominal aorta respectively). This disparity in the increase of the variability indicates that, although these three arteries are subjected to a slightly bigger reduction of the mean flow, they are also able to counteract more efficiently the increase in variability induced by the AF, ensuring a more stable perfusion.

The differences in the decrements between the beat-averaged pressure and flow rate values are likely due to the pressure regulatory mechanisms included in the model, which adapt resistances, compliances, and heart rate to maintain the target mean arterial pressure.

Focusing on the pulse pressures, we see, in all the sites, a

marked reduction in the mean value, which can be attributed mainly to the decrease in the SV. We recall that the pulse pressure is one the most important – but at the same time difficult to evaluate at distal sites – hemodynamic parameters as it is thought to be the main marker of vascular aging [14], cognitive impairment [15], and debilitating conditions such as glaucoma [16]. The pulse pressure is seen to decrease the most in the aortic root (-30.6%). On the contrary, as we move to the distal branches, the reduction in pulsatility becomes less pronounced as the smallest reduction is observed in the superior mesenteric artery (-25.9%). All the tracts present an increase in the std value of the PP, with the highest increment found in the abdominal aorta (+147.1%). As observed for the SV, the increased std associated with the strong reduction of the mean value leads to a scenario in which the pulse pressure of all six sites rarely reaches physiological values.

IV. CONCLUSION

This study employed a multiscale cardiovascular model to investigate gastrointestinal perfusion in AF conditions. Multiscale reduced order models represent the best balance between level of description and computational cost, allowing the study of large regions of the body circulation. In contrast, three-dimensional CFD approaches are more computational demanding and suitable for focusing on small portions of vessels, such as aneurysms or localized vessel pathologies.

The irregular organ perfusion and the higher exposure to extreme flow rate and pressure values induced by AF could be symptomatic of local suffering or dysfunction at the abdominal level in the long-term. In fact, AF is known as a predisposing risk factor for acute mesenteric ischemia [4]. Although this augmented risk can be mainly related to embolism formation [17], AF patients have a high likelihood of being found with abdominal pathology, such as arterial hemorrhage [18]. Moreover, AF reduces ventricular contractility and CO, leading to a reduction of renal perfusion which in turn can further impair kidney function of patients with chronic kidney disease [5].

Awaiting deeper clinical examination in the future, present results suggest that anomalous pressure levels might be related to hemorrhagic events, while reduced blood flow repartition can locally alter organ perfusion, thus impairing physiological function and accelerating progression of already present pathologies.

ACKNOWLEDGEMENT

This study was carried out within the 2022EAN2BB "Cerebral fluid dynamics: investigating the association between atrial fibrillation and dementia through an integrated in silico-in vivo framework" project – funded by the Ministero dell'Università e della Ricerca – within the PRIN 2022 program (D.D.104 - 02/02/2022). This manuscript reflects only the authors' views and opinions and the Ministry cannot be considered responsible for them.

REFERENCES

- [1] G. A. Roth, et al., Global burden of cardiovascular diseases and risk factors, 1990-2019: Update from the gbd 2019 study, *J. Am. Coll. Cardiol.* 76(25) (2020) 2982–3021.
- [2] G. Hindricks, et al., 2020 ESC guidelines for the diagnosis and management of atrial fibrillation developed in collaboration with the European association for cardio-thoracic surgery (EACTS), *Eur. Heart J.* 42(5) (2021) 373–498.
- [3] V. Jacobs, M. J. Cutler, J. D. Day, T. J. Bunch, Atrial fibrillation and dementia, *Trends Cardiovasc. Med.* 25(1) (2014) 44–51.
- [4] Klar E, Rahmanian PB, Becker A, Hauenstein K, Jauch KW, Luther B (2012) Acute mesenteric ischemia: A vascular emergency. *Deutsches Arzteblatt International* 109(14):249-256.
- [5] Kim, S.-M., et al., Association of Chronic Kidney Disease With Atrial Fibrillation in the General Adult Population: A Nationwide Population-Based Study, *J. Am. Heart Assoc.*, 12(8), e028496.
- [6] M. Fois, A. Diaz-Artiles, S. Y. Zaman, L. Ridolfi, S. Scarsoglio, Linking cerebral hemodynamics and ocular microgravity-induced alterations through an in silico-in vivo head-down tilt framework, *npj Microgravity* 10(1) (2024) 22.
- [7] S. Scarsoglio, A. Guala, C. Camporeale, and L. Ridolfi, "Impact of atrial fibrillation on the cardiovascular system through a lumped-parameter approach," *Med Biol Eng Comput*, vol. 52, no. 11, pp. 905–920, Nov. 2014.
- [8] S. Scarsoglio, C. Gallo, L. Ridolfi, Effects of atrial fibrillation on the arterial fluid dynamics: A modelling perspective, *Meccanica* 53 (13) (2018) 3251–3267.
- [9] S. Scarsoglio, C. Camporeale, A. Guala, L. Ridolfi, Fluid dynamics of heart valves during atrial fibrillation: a lumped parameter-based approach, *Comput. Methods Biomech. Biomed. Engin.* 10(19) (2016) 1060–1068.
- [10] S. Scarsoglio, A. Saglietto, F. Gaita, L. Ridolfi, M. Anselmino, Computational fluid dynamics modelling of left valvular heart diseases during atrial fibrillation, *PeerJ* 4 (2016) e2240.
- [11] C. Gallo, L. Ridolfi, and S. Scarsoglio, "Cardiovascular deconditioning during long-term spaceflight through multiscale modeling," *npj Microgravity*, vol. 6, no. 1, p. 27, Oct. 2020.
- [12] M. Fois, S. V. Maule, M. Giudici, M. Valente, L. Ridolfi, and S. Scarsoglio, "Cardiovascular Response to Posture Changes: Multiscale Modeling and in vivo Validation During Head-Up Tilt," *Front. Physiol.*, vol. 13, p. 826989, Feb. 2022.
- [13] A. Guala, M. Scalseggi, and L. Ridolfi, "Coronary fluid mechanics in an ageing cardiovascular system," *Meccanica*, vol. 52, no. 3, pp. 503–514, Feb. 2017.
- [14] O'Rourke, M.F., Hashimoto, J., 2007. Mechanical Factors in Arterial Aging. *Journal of the American College of Cardiology* 50, 1–13.
- [15] Stefansdottir, H., Arnar, D.O., Aspelund, T., Sigurdsson, S., Jonsdottir, M.K., Hjaltason, H., Launer, L.J., Gudnason, V., 2013. Atrial Fibrillation is Associated With Reduced Brain Volume and Cognitive Function Independent of Cerebral Infarcts. *Stroke* 44, 1020–1025.
- [16] Zaleska-Żmijewska, A., Janiszewski, M., Wawrzyniak, Z.M., Kuch, M., Szaflik, J., Szaflik, J.P., 2017. Is atrial fibrillation a risk factor for normal-tension glaucoma? *Medicine* 96, e8347.
- [17] Hazanov N, et al. (2004) Acute Renal Embolism: Forty-Four Cases of Renal Infarction in Patients With Atrial Fibrillation. *Medicine* 83(5): 292-299.
- [18] Hunt SJ, Coakley FV, Webb EM, Westphalen AC, Poder L, Yeh BM (2009) Computed tomography of the acute abdomen in patients with atrial fibrillation. *J Comput Assist Tomogr* 33(2):280-5.